Al-Azhar Engineering 16th International Conference

Vol. 19, No. 72, July 2024, 183 - 201

A COMPARATIVE STUDY OF MODULE EFFICIENCY AND SIZING OF THE INVERTER'S LCL FILTER FOR PHOTOVOLTAIC SYSTEMS: A CASE STUDY

Mohamed. M. Reda[1*], Mohamed I. Elsayed[2], M.A. Moustafa Hassan[3], Hatem Seoudy[4]

[1]Electrical and Electronic Engineering Department, Faculty of Engineering, May University, 15th May City, 11235, Cairo, Egypt

[2]Electrical Engineering Department, Faculty of Engineering, Al-Azhar University, Nasr City, 11884, Cairo, Egypt

[3]Electrical Engineering Department, Faculty of Engineering, Cairo University, Giza City, 12613, Cairo, Egypt

[4]Electrical power and machine Department, The Higher Institute of Engineering, Elshorouk city,11837, Egypt

***Correspondence:** Mohamed.Mohamady@muc.edu.eg

Citation:

M.M. Reda, M.I. Elsayed, M.A.M. Hassan and H. Seoudy, "a comparative study of module efficiency and sizing of the inverter's lcl filter for photovoltaic systems: a case study" Journal of Al-Azhar University Engineering Sector, vol. 19, pp. 183 - 201, 2024.

Received: 07 November 2023

Revised: 15 December 2023

Accepted: 20 December 2023

DoI:10.21608/auej.2023.251916.1493

ABSTRACT

This study examined three PV models—polycrystalline, monocrystalline, and thin film—at their suitable inclination angles, monitoring radiation and ambient temperature to compare their performance in summer and winter emphasis on the real case study situated at Faculty of Engineering, Heliopolis University. The study examined two angles with variable steel structures. A detailed comparison done by putting modules at a 15-degree angle in 2021 and a 30-degree angle in 2022. A 15º inclination angle is better in winter than a 30º, but a 30º is better in summer, according to this study. A comparison analysis was performed to assess the dimensions of the output filter for inverters employed in three solar systems. This study utilizes Genetic Algorithm (GA) and Water Cycle Algorithm (WCA) to examine the sizing of the LCL output filter of the inverter. Additionally, the research investigated the critical aspect of determining the optimal size of the output filter inverter, with a primary focus on analyzing the Levelized Cost of the Electricity generated (LCOE)

KEYWORDS Photovoltaics, Genetic Algorithms, Water Cycle Algorithms, Inclination angle, LCL Filter.

مقارنة لكفاءة الوحدة الشمسية وتحديد حجم مرشح LCL العاكس الخاص بأنظمة الطاقة الشمسية: دراسة حالة

محمد محمد رضا[1*]، محمد إبراهيم السيد[2]، محمد مصطفي احمد[3]، حاتم سعودي[4]

[1] قسم كهرباء واليكترونيات، كلية الهندسة، جامعة مايو، مدينة 15 مايو، 11235، القاهرة، مصر.
[2] قسم كهرباء، كلية الهندسة، جامعة الازهر، مدينة نصر، 11884، القاهرة، مصر.
[3] قسم كهرباء، كلية الهندسة، جامعة الازهر، مدينة الجيزة، 12631، القاهرة، مصر
[4] قسم كهرباء قوي وآلات كهربية، المعهد العالي هندسة الشروق، مدينة الشروق، 11873، القاهرة، مصر.

***البريد الاليكتروني للباحث الرئيسي:** Mohamed.Mohamady@muc.edu.eg

الملخص

تناولت هذه الدراسة ثلاث نماذج للخلايا الشمسية - البلورية، والأحادية البلورية، والرقيقة – بالأخذ في الاعتبار زوايا الانحناء المناسبة لها، حيث تم مراقبة الإشعاع ودرجة الحرارة المحيطة لمقارنة أدائها في فصلى الصيف والشتاء، بدراسة الحالة الواقعية

الموجودة في كلية الهندسة بجامعة هليوبوليس. وقد تم دراسة زاويتان مختلفتان باستخدام هياكل متنوعة، حيث تمت المقارنة التفصيلية عن طريق تثبيت الوحدات بزاوية 15 درجة في عام 2021 وبزاوية 30 درجة في عام 2022. ووفقًا لهذه الدراسة، يعتبر زاوية الانحناء 15 درجة أفضل في الشتاء من زاوية 30 درجة، ولكن زاوية 30 درجة تظهر أفضل أداء في الصيف. تم إجراء مقارنة لتقييم عناصر مرشح إخراج العاكس المستخدم في ثلاثة أنظمة شمسية. تعتمد هذه الدراسة على خوارزميات الجينات الوراثية (GA) وخوارزمية دورة المياه (WCA) لفحص قيم مرشح الإخراج LCL للعاكس. بالإضافة إلى ذلك، قام البحث بتحديد الحجم الأمثل لمرشح الإخراج في العاكس، مع التركيز على تحليل تكلفة الكهرباء المولدة (LCOE).

الكلمات المفتاحية: الخلايا الشمسية، الخوارزميات الوراثية، خوارزميات دورة المياه، زاوية الميل، مرشحLCL .

1. INTRODUCTION

Photovoltaic (PV) systems are often regarded as the forefront of energy technology, among a diverse array of ongoing renewable and clean energy initiatives worldwide. The primary objective of this technology is to generate electricity from solar radiation in a manner that is economically competitive and perhaps superior to alternative energy sources. A comparative analysis is required to address the challenges associated with PV diffusion. This examination should encompass economic, technical, operational, and institutional perspectives [1]. Currently, there exist three distinct categories of photovoltaic modules that are fabricated using crystalline silicon as their primary material. These categories include monocrystalline silicon, polycrystalline silicon, and thin film [2].

Various variables have been identified as affecting the performance of photovoltaic systems. The parameters to be considered include the amount of solar energy collected by the solar modules, the ambient temperature, and the inclination angle. There are various advantages associated with those systems. Firstly, they are environmentally friendly, producing no noise or pollution. Secondly, they offer flexibility and can be adapted to various applications. Thirdly, they have no moving parts, making them highly reliable and long-lasting, with minimal maintenance required. Additionally, they provide energy independence, as they rely on the free and readily available energy source of sunlight. Furthermore, the costs of PV systems are generally decreasing, while conventionally produced electricity is expected to become more expensive. This makes them a viable option for covering against future energy price increases. Although they offer numerous advantages, they also have certain drawbacks. These include a higher initial cost compared to other power-generating technologies, the need for a relatively large array area to generate a substantial amount of power, the dependence on the availability of solar radiation resources at a specific location to determine the feasibility of power production, and limited or insufficient knowledge about the potential of solar PV systems in certain regions [3]. PV systems that are connected to the electrical grid utilize a transformer-less, full-bridge direct current to alternating current converter. In contrast to PV inverters with galvanic isolation, transformer-less PV inverters offer several advantages, including reduced cost, increased efficiency, and decreased weight [4, 5]. The utilization of an LCL-type output filter, as opposed to conventional L or LC-type filters, is intended to enhance the power density of the photovoltaic (PV) inverter [6]. To enhance the power density of PV inverters, the utilization of LCL-type output filters is preferred over L- or LC-type filters [7].

A cost-effective deployment of PV systems connected to the grid can be achieved by minimizing the initial investment cost in order to achieve a cost-effective deployment of photovoltaic (PV) systems that are connected to the grid, it is important to minimize the initial investment cost associated with purchasing and installing the various components of the PV system, such as PV modules and inverters. Additionally, maximizing the amount of energy that is injected into the electric grid and ensuring the reliability of the system are crucial. This can be achieved by minimizing any malfunctions that may occur in the PV system components throughout its operational lifetime period[8-10]. The objective of the optimization approach for PV inverter sizing encompasses the optimization of both the converter circuit and the circuit-device levels. The proposed methodology considers the solar irradiation potential of the installation site. It also considers the impact of the operational characteristics of the array on the design of grid-connected inverters. Additionally, it takes into consideration the restrictions imposed by electric grid regulations and standards [11].

This study will utilize empirical data obtained from an actual system that has been deployed in Heliopolies university in Cairo. The system has three distinct types of photovoltaic modules, with each kind being connected to a separate inverter. Typically, the array consists of a minimum of eight modules, with ground mounting being the preferred option in most cases. The primary topic of interest pertains to the aerodynamic force exerted by wind on the array. The peak energy consumption of a building may not align with the peak production of PV system, as indicated by previous research [12]. This research has two primary objectives: firstly, to evaluate several photovoltaic (PV) modules at their ideal inclination angle, which was achieved by a comprehensive test that included monitoring of radiation and ambient temperature. The study compared summer and winter conditions over a two-year period (2021 and 2022) by analyzing the effects of two distinct angles (15 degrees and 30 degrees) utilizing varied steel structures. In order to do this, modules are positioned at a 15-degree angle over the entirety of 2021, and at a 30-degree angle for the entirety of 2022. The comparison is then conducted. The other aspect of this research is determining the appropriate size of the output filter inverter and analyzing the levelized cost of energy (LCOE) as the primary objective function. The LCOE is a crucial component in assessing the cost of renewable energy. Two optimization approaches, Genetic Algorithm (GA) and Water Cycle Algorithm (WCA), have been applied to reduce the Levelized Cost of Energy (LCOE). This paper presents a case study that examines a specific place, Heliopolies university, by analyzing relevant facts and discussing the established ruler's jurisdiction within this region. The rest of the article is organized as Section 2 presents material and methods; Section 3 discusses the results. Section 4 conclusion.

2. Materials and Methods

2.1. The installed system under study.

The system under investigation can be categorized into two primary portions, Section 2.1.1 and Section 2.1.2. Section 2.1.1 provides an overview of the load calculation methodology employed for the system under investigation as well as detailed descriptions of the system itself. Section 2.1.2 looks at the techniques used to calculate the output power that the system produces under various operational scenarios.

2.1.1. Load calculation of the system

Fig. 1. Faculty of engineering

This study describes a real case study above the roof of faculty of engineering at Heliopolis university for sustainable development in **Fig. 1**. where are three different PV modules are equally installed in same, place and same weather conditions. This study endeavors to develop a photovoltaic (PV) system that can supply the requisite electrical power to various facilities such as laboratories, conference rooms, classrooms, offices, and computer rooms. The aggregate electrical power consumption required for lighting purposes amounts to approximately 4.5 kilowatts, excluding the air conditioning units.

The insolation value, which represents the quantity of beneficial sunlight accessible to PV panels under the most unfavourable conditions of the year, is utilized for analytical purposes to guarantee year-round operational efficiency of the system. In tested area, the average duration of sun insolation for the month of the year is recorded to be 6.0 hours each day. The data shown in Table1. indicates a notable occurrence of solar energy in the specified region, particularly during year as measured in this test presented, the average daily radiation is recorded at 8.01 kWh/m2/day.

Table 1. The monthly average values of daily solar radiation (kWh/m/day) in tested area.

Month	**Daily Radiation in kWh/m^2/day**
January	3.18
February	4.30
March	5.60
April	6.68
May	7.39
June	8.01
July	7.93
August	7.36
September	6.34
October	4.93
November	3.73
December	2.96

`

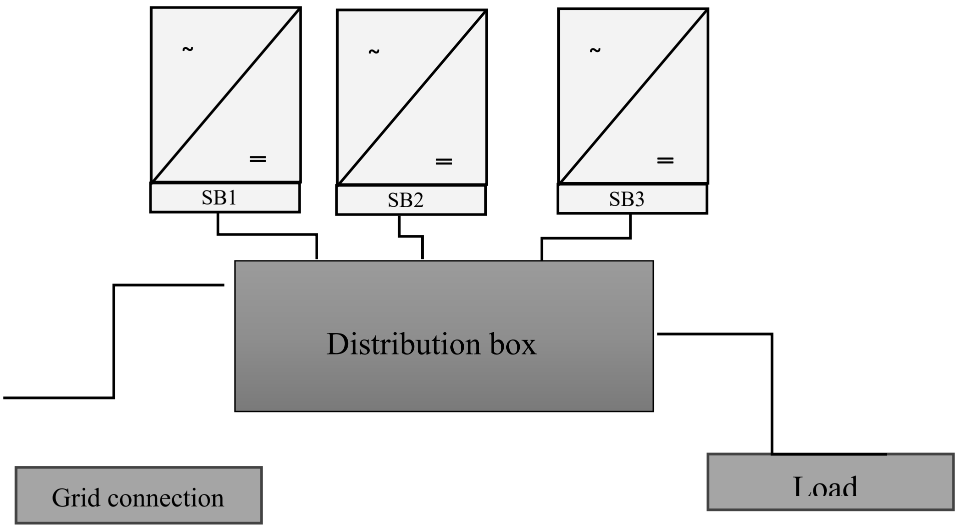

Fig. 2.Schematic for the power network

This test, including the three different types of solar panels, is shown in Fig. 2. each type is connected to an inverter: SB1 is connected to polycrystalline modules, SB2 is connected to monocrystalline modules, and SB3 is connected to thin film modules.

2.1.2. Summary of measurements in 2021-2022 with two different angles.

The system is equipped with a monitoring system that displays statistics on output power, AC voltage, DC voltage, and current output. The data from the system's inverters can be collected by utilizing a web interface. Additionally, the system incorporates various sensors to assess the impact of environmental variables on the comparison and design process.

Fig. 3.Meto-Sation

Fig. 4. sensor box collector

For instance, a Meto-station in Fig.3. device is utilized to gather data on ambient temperature and irradiation. The measurement is conducted by employing a sensor box collector in Fig.4., whereby all the sensors are interconnected with the gateway through an internet connection. The data stored in the portal enables convenient comparisons among the three types of PV systems in terms of efficiency, optimal environmental conditions, and economic considerations. The recorded outcomes, obtained from measurements acquired from the portal, are utilized to assess, and compare the performance of each kind and the overall performance of the system. The subsequent figures (Figures 2–9) present the empirical measurement data obtained in the summer and winter of 2021 and 2022 with two different inclination angles of 15 degrees and 30 degrees, respectively, when the load was imposed. The numerical values are obtained immediately as the resulting data from data recorders. The figures presented illustrate the correlation between irradiance and inclination angle.

Case 1: In summer with inclination angle 15º and 30º

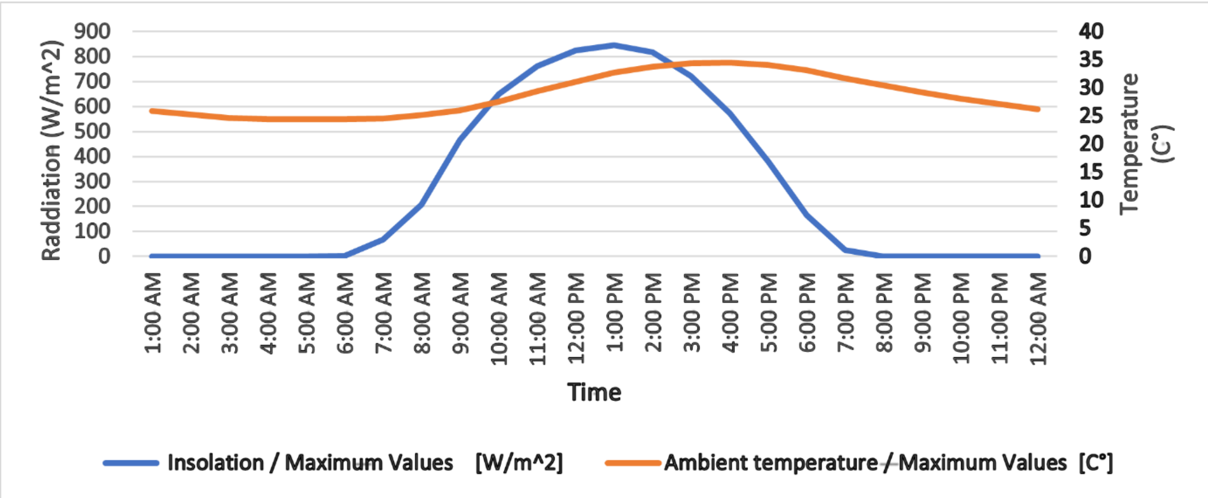

Fig. 5. The Radiation data in summer with inclination angle 15º in 2021

In the following **Fig.5.** it is shown that the maximum radiation value is 844.813 W/m^2 in summer 2021with inclination angle 15º.

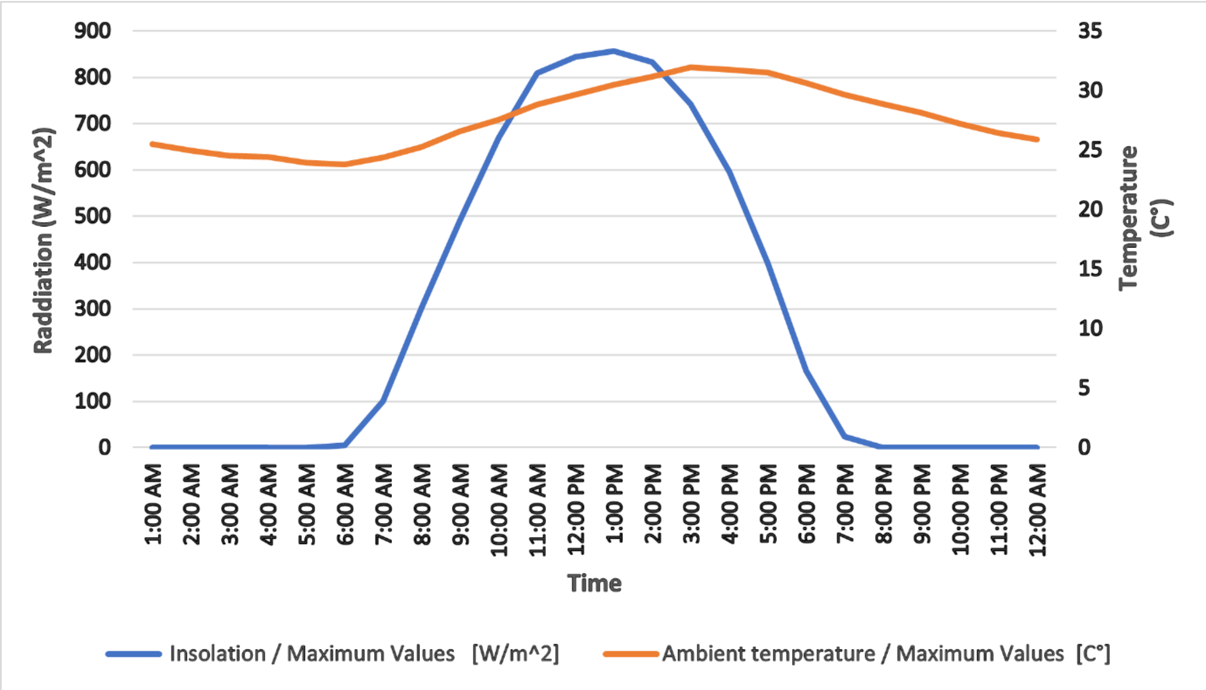

Fig. 6. The Radiation data in summer with inclination angle 30^o in 2022

In **Fig.6**. seen the radiation in summer 2022 with angle 30º raised up to 876.076 W/m2 compared to the value of radiation with angle 150 in Fig.5. in addition, from Fig.5. and Fig.6. the temperature in this summer is almost the same. This change in radiation will effect in power output.

Case 2: In winter with inclination angle 15^o and 30^o.

The average radiation and temperature were recorded with inclination angle 15^0 in 2021 and with inclination angle 30^0 in 2022 at the same environmental conditions.

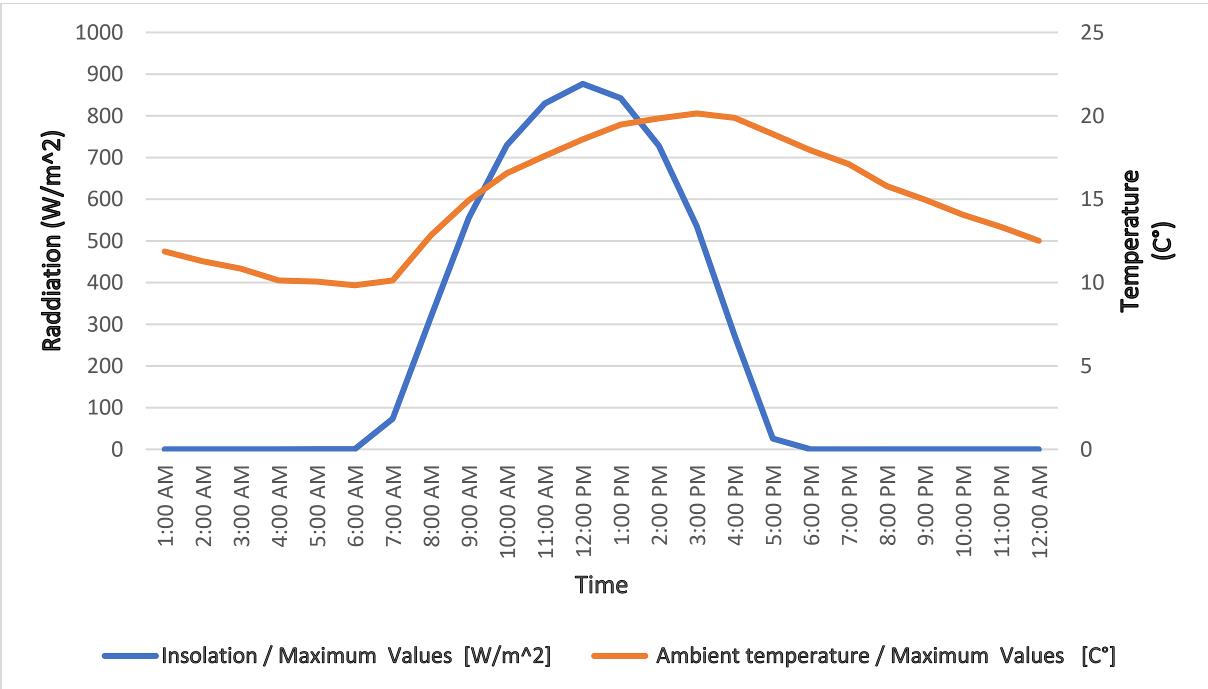

Fig. 7.The Radiation data in winter with inclination angle 15^o in 2021

In **Fig.7.** with the same temperature the radiation increased to 866.706 W/m^2 this value is very close to the radiation value in summer with angle 30^0 in 2022.

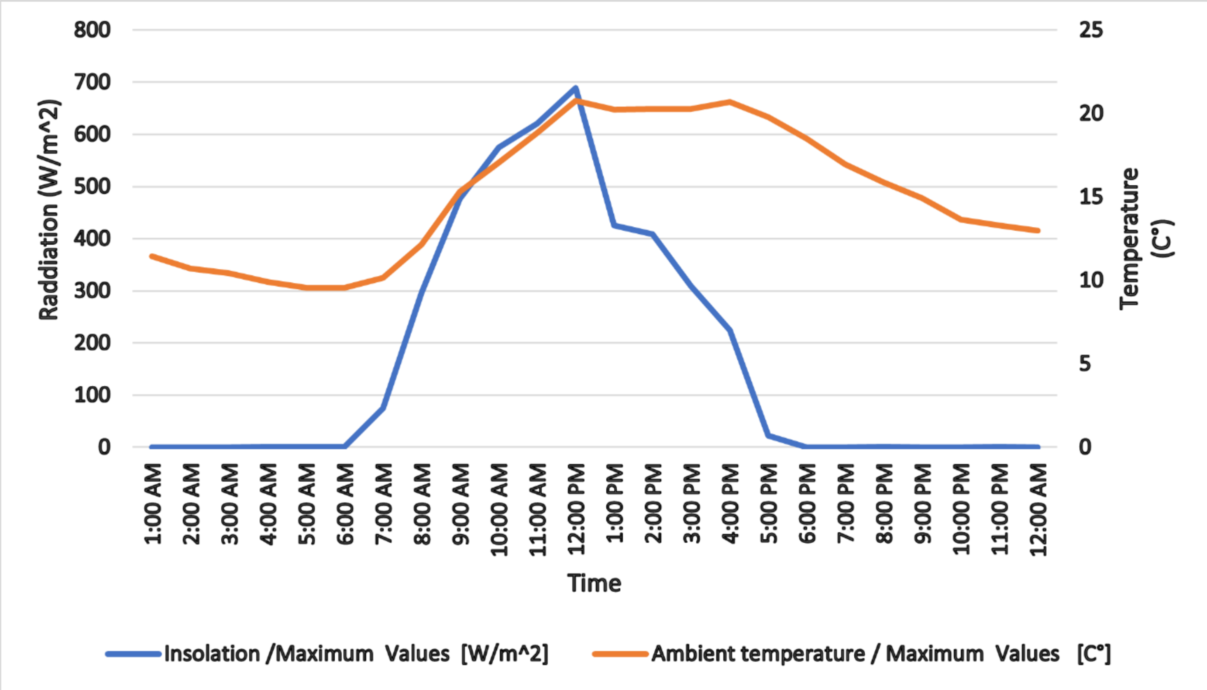

Fig. 8. The Radiation data in winter with inclination angle 30º in 2022

In **Fig.8.** In winter the radiation decreased to 688.949 W/m^2 because of the change of inclination angle. The alteration of the angle during winter, from 15^0 to 30^0 degrees, has a significant impact on the efficiency of radiation collection at PV modules. Consequently

2.2. The PV inverter power density, LCL type output filter

The proposed methodology involves the calculation of the voltage and power output of the PV array on an hourly basis over the course of one year. The PV inverter control unit is responsible for executing the MPPT process, which aims to optimize the power output of the PV system by ensuring that the maximum power available from the PV panels is sent to the PV inverter. The power output of the PV array at time t ($1 \le t \le 8760$), denoted as $P_{Pv,t}$ (W), and also equivalent to the input power of the PV inverter, is determined by the analysis of the PV modules model[13, 14].

The output of the inverter will be influenced by the solar irradiation and ambient temperature time-series, as well as the electrical specifications of the PV modules and their configuration (i.e., connection in series or parallel) within the PV array. These inputs are incorporated into the proposed optimization procedure by the PV inverter designer. The output current $I_{o,t}$ of the photovoltaic (PV) inverter at a certain hour t (where t ranges from 1 to 8760) is determined by the utilization of the power balance equation.[11]:

$$P_{pv} = P_{tot,t} + V_n . I_{o,t} \qquad (1)$$

$$P_{tot} = P_{cond} + P_{sw} + P_d + P_{Lc} + P_{Lr} + P_{cu} \qquad (2)$$

where $P_{tot,t}$ is the PV inverter total power loss at hour t ($1 \le t \le 8760$). The value of $I_{o,t}$ is obtained in (1) using a numeric analysis method .The PV inverter total power loss, P_{tot} (W), is equal to the sum of the IGBTs and anti-parallel diodes conduction and switching losses, P_{cond} (W) and P_{sw} (W), respectively, the power loss on the LCL filter damping resistor, P_d (W), the LCL filter inductors core and winding losses, $P_{L,c}$ (W) and $P_{L,r}$ (W), respectively, and the control unit power consumption (due to the circuits of the SPWM modulator, IGBT drivers, sensors and signal conditioners etc.), P_{cu} (W). The values of P_{cond} and P_{sw} are calculated using the power loss model presented in[15].

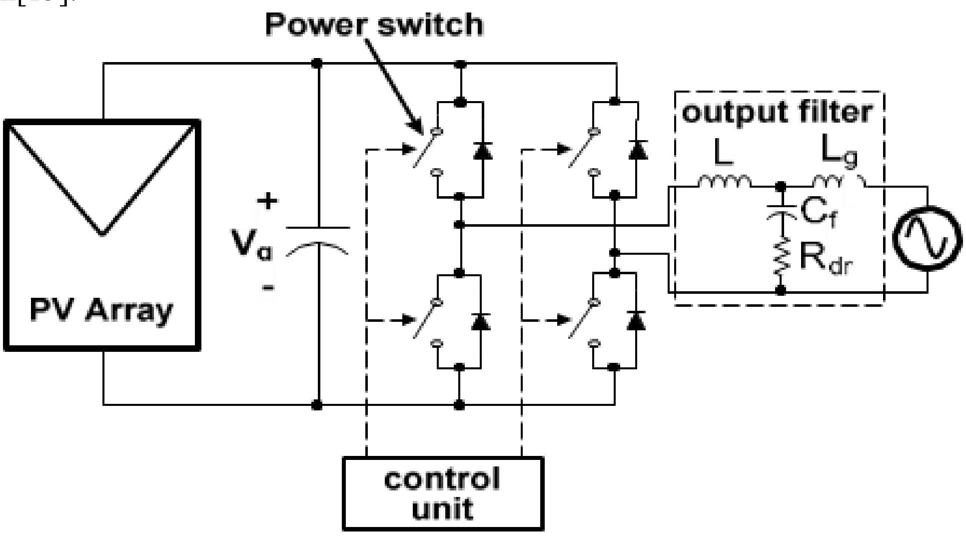

Fig. 9 . PV system connected to the grid with LCL output filter.[16]

Fig.9. PV system connected to the grid engaging a transformer-less PV inverter.

The objective of the suggested design is to optimize the calculation of the ideal values for the PV inverter switching frequency, Fs, as well as the output filter components and the optimal types of power semiconductors. Referring to Figure 10, the vector X, which represents the design variables of the optimization problem, is in the form of $X=[L|L_g |C_f | F_s]$ [16].

The determination of the ideal value for the damping resistor, R_{dr}, in the LCL filter is performed by utilizing the optimal values obtained for L, Lg, and Cf, as previously analysed in[17]. The damping resistor value, R_{dr} (Ω), is set equal to the filter capacitor impedance at the resonant frequency F_{res}[17]:

$$R_{dr} = \frac{1}{2\pi\, C_f F_{res}} \quad (3)$$

$$P_d = [\left(2\pi V_n\, C_f\right)^2 + {I_r}^2]R_{dr} \quad (4)$$

2.3. Optimal inverter sizing.

The objective of designing the PV inverter power density, LCL-type output filter is to minimize the Levelized Cost of the Electricity generated'' (LCOE).

$$\underset{X}{minimize}\{LCOE(X)\} = \underset{X}{minimize} \quad (5)$$

where $C_m(X)$ (€) is the manufacture cost and E_y (X) (Wh) is the power injected into the grid during a year. This paper shows an algorithm for economical design of PV systems based on the specifications of available inverters [17].

$$E_y = \sum_{t=1}^{8760} v_n\,.I_{o,t}.\Delta t \quad (6)$$

$$C_m(X) = C_{inv.}P_n + C_i\left(L + L_g\right)\frac{P_n}{V_n} + C_r.R_{dr} + SF.P_{d,max} \quad (7)$$

Where Δt is the time step set to Δt=1, C_{inv} (€/W) is the PV inverter manufacturing cost without including the cost of the LCL filter components, C_i [€ / (H A)] is the filter inductors cost per unit inductance and current, cc (€/F) is the filter capacitor cost per unit capacitance, C_r [€/ Ω.W] is the filter damping resistor cost per unit resistance and power, SF (%) is the damping resistor over-sizing factor and $P_{d,max}$ (W) is the maximum power dissipated on the damping resistor during the year.

2.4. Water Cycle Algorithm (WCA)

The application of the "Water Cycle Algorithm" (WCA) will yield the most optimal design of Levelized Cost of Electricity (LCOE). The water cycle algorithm (WCA) has gained recognition due to its utilization of observations pertaining to the water cycle process and the flow of rivers and streams towards the ocean. This algorithm is classified as a population-based metaheuristic algorithm. In recent times, there has been a noticeable increase in the number of applications utilizing the Whale Optimization Algorithm (WCA), which has found utility across various domains of optimization.

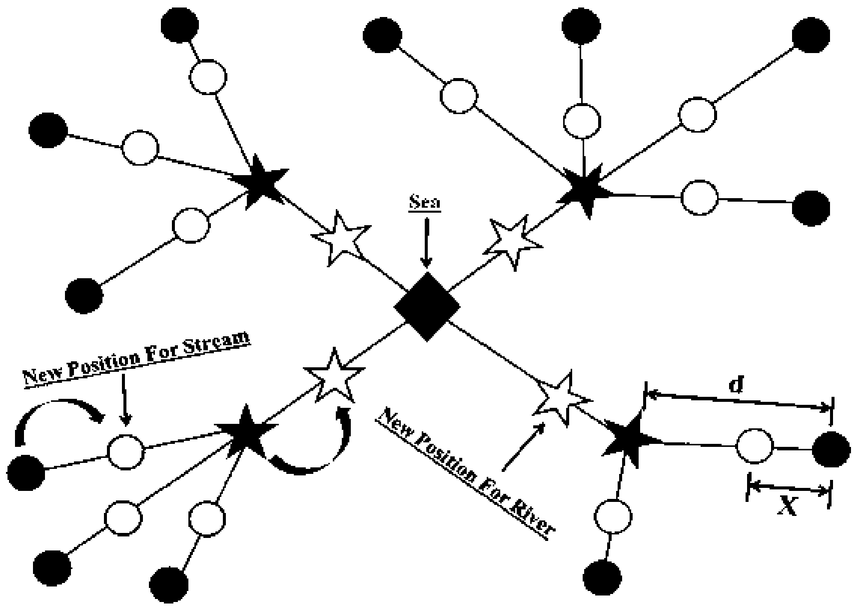

Fig. 10.A schematic view of the approaches used in the WCA[18].

The WCA optimization method is guided by **Fig11**, which represents circles, stars, and a diamond symbolizing streams, rivers, and the sea, respectively. The white, vacant figures represent the updated locations occupied by streams and rivers. Furthermore, the original WCA incorporates the processes of evaporation and precipitation in order to boost its overall potential.

To provide further clarity, the concept of evaporation functions in a manner akin to mutation in genetic algorithms (GAs), leading the algorithm to move away from local optima. Indeed, this notion allows the algorithm to avoid premature convergence towards local optima. Evaporation is the primary mechanism by which sea water undergoes vaporization, occurring concurrently with the inflow of rivers and streams into the ocean[18, 19].

The maximum value, denoted as d max, is a numerical quantity that is relatively small and in close proximity to zero. Following the process of evaporation, precipitation occurs, leading to the formation of new streams in various geographical regions. To determine the precise locations of the newly formed streams, a higher value of d_{max} restricts the number of searches conducted, while smaller values promote a greater focus on searching near the sea.

Hence, the parameter d max regulates the level of search intensity in proximity to the ocean. The maximum value of d decreases adaptively in the following manner[20, 21]:

$$d_{max}(t+1) = d_{max}(t) - \frac{d_{max}(t)}{Max.iteraion} \quad (8)$$

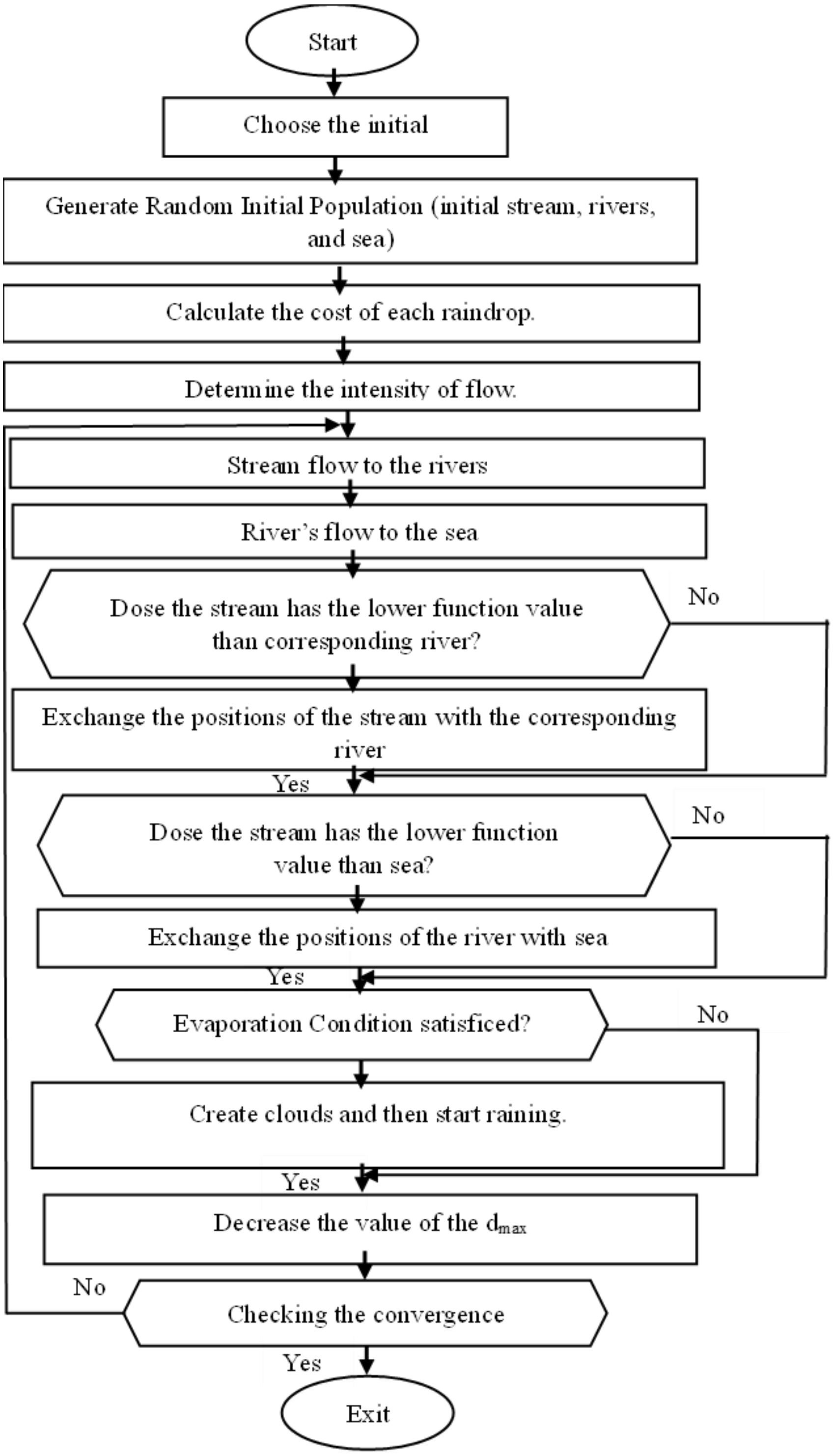

Fig. 11. The flow-chart of the needed optimization procedure WCA[20]

Fig.11 depicts a flowchart outlining the requisite automated optimization stages. The inputs to the optimization algorithm are as follows:

The device datasheet provides information regarding the price and device-specific properties of the power semiconductors utilized in constructing the inverter. These parameters determine the switching and conducting behaviours of the power semiconductors. The present study focuses on the examination of the price and technical specifications of magnetic components and capacitors that are readily accessible in the market. These components are intended for utilization in the building of the output filter. The relevant information regarding these components can be found in their respective datasheets.

The discussion encompasses the circuit topology and specifications of PV inverters, including power rating, input and output voltage ranges, and output frequency. Additionally, it addresses the maximum allowable harmonic current levels as stipulated by grid codes and international standards. Furthermore, it explores the operational characteristics of PV modules, such as power rating and open-circuit voltage, as well as their configuration within the PV array. Lastly, it considers the time-series data of 1-hour average solar irradiance and ambient temperature throughout the year[12].

3. RESULTS AND DISCUSSION

The first part of this section is the corresponding power with different inclination angle with respect to the three different types of PV while SB 1 is Polycrystalline modules, SB 2 is monocrystalline modules and SB 3 is the thin film modules.

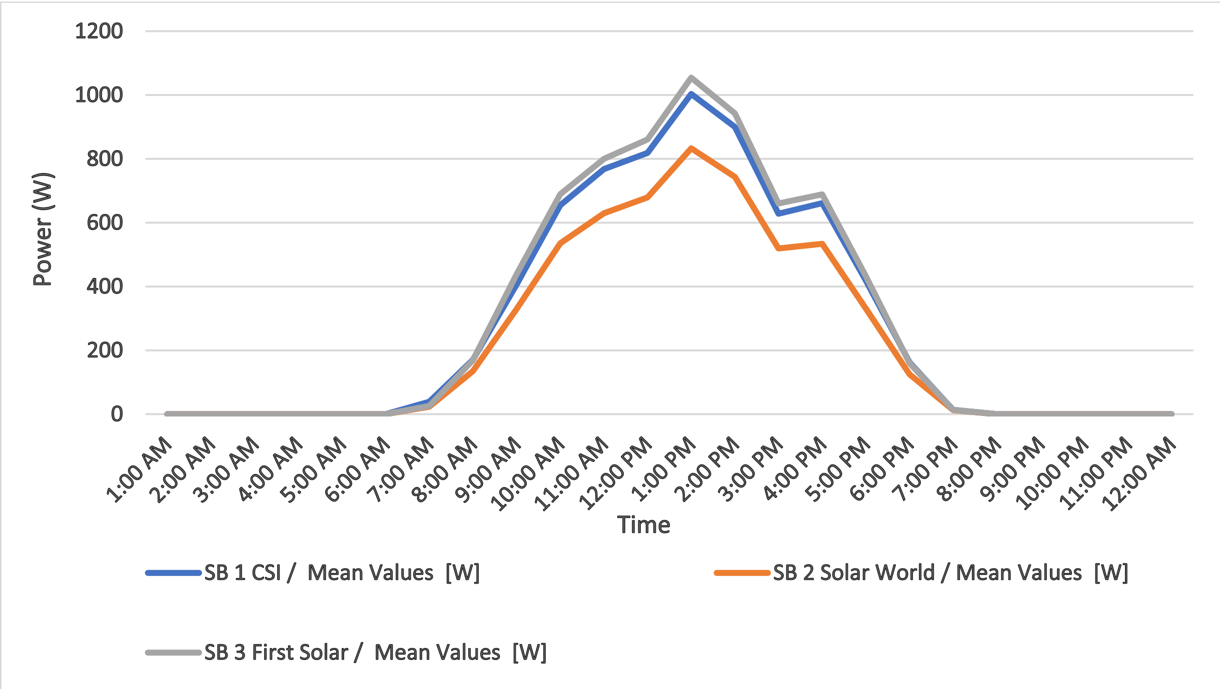

Fig. 12. The power data in summer with inclination angle 15°

shown in **Fig.12.** the (Polly crystalline) modules are the highest power output than the (Monocrystalline) modules but the lowest power output was from the (Thin Film) modules.

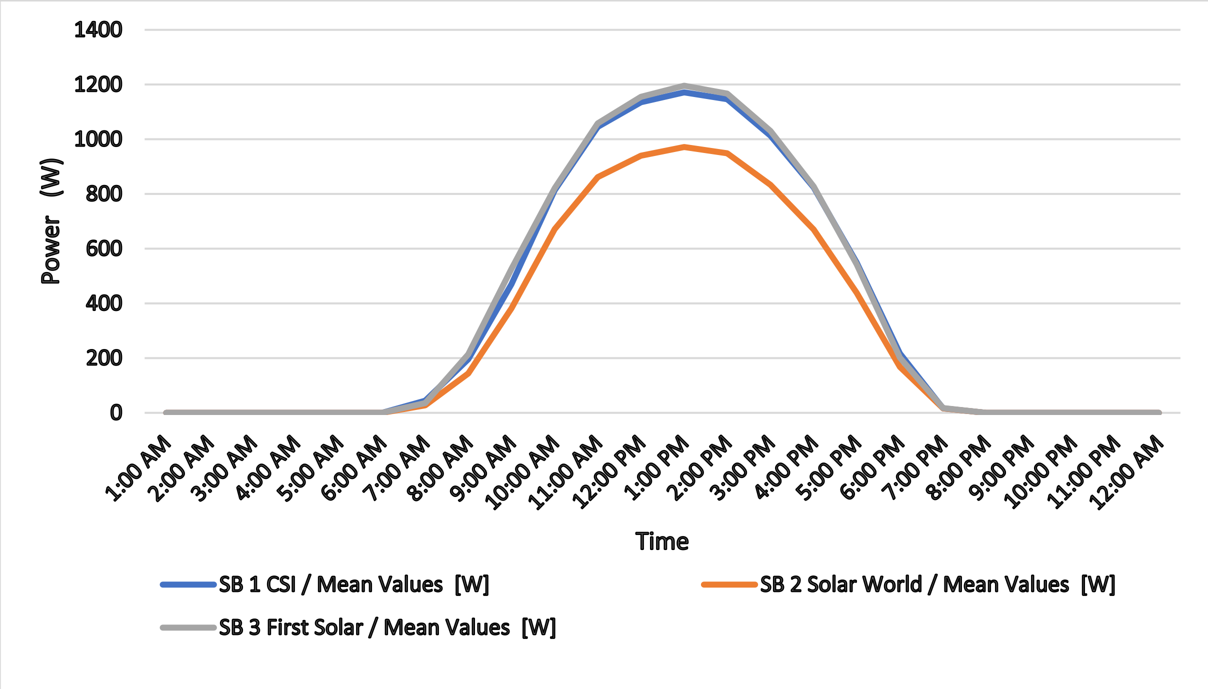

Fig. 13.The power data in summer with inclination angle 30°

In **Fig.13** the power output in three types increased compared to **Fig.12.**with angle 30^0 because of changing in radiation value. This research conducted throughout the summer season provided insights into the optimal inclination angle, which was found to be 30^0 degrees. However, it is crucial to do a similar study during the winter season in order to observe variations in power output based on the inclination angle.

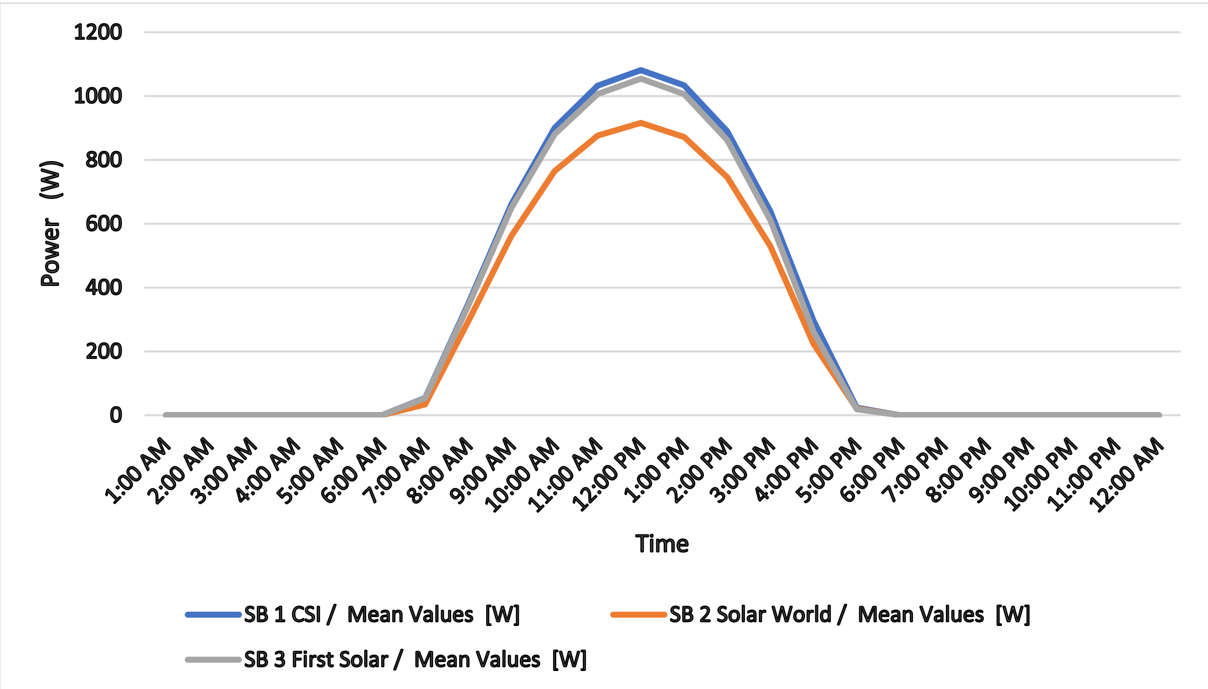

Fig. 14. The power data in winter with inclination angle 15°

It can be seen from **Fig.14.** that under clouds the total output power of the system is very close to the output power of the system in summer.

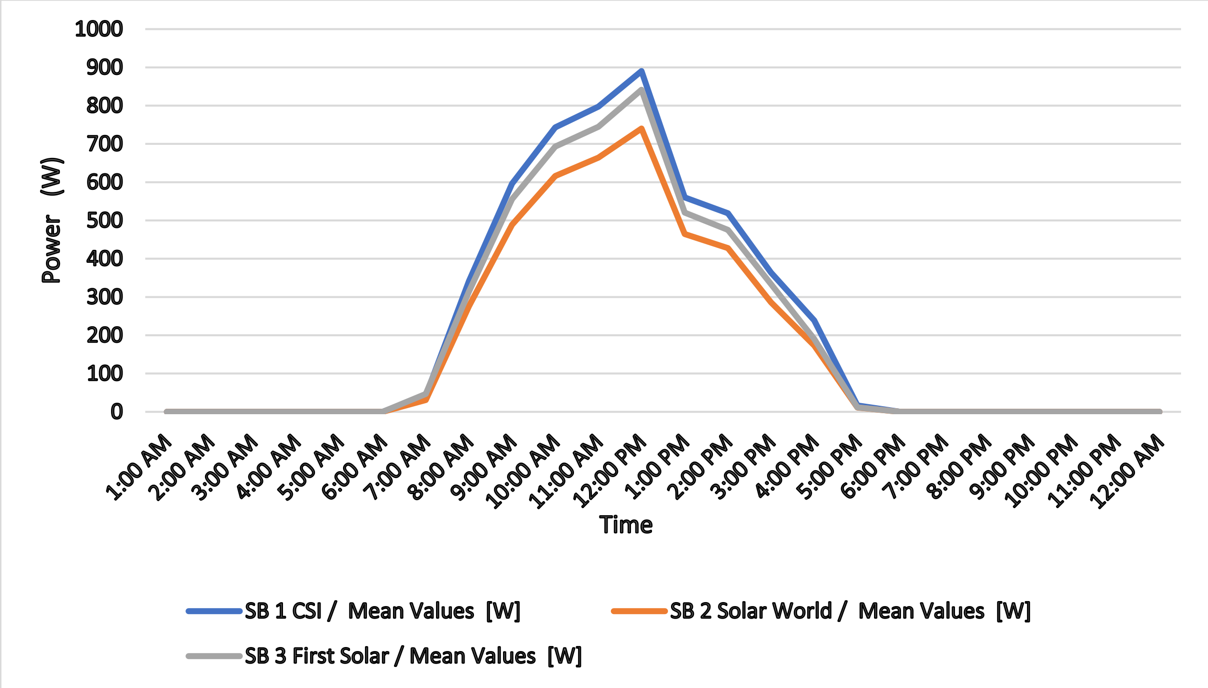

Fig. 15. The power data in winter with inclination angle 30°

It can be seen from **Fig.14.** that under clouds the total output power of the system decreases by 25 % compared to the power output in summer.

As shown from **Fig.15.**the power raised up than **Fig.14**.based on the findings of winter study, it is evident that an inclination angle of 15° during winter yields a power output that closely approximates the power output observed during summer at an inclination angle of 30°, as observed in instance.

Table 2. Summary of the results for the three types with respect to temperature and inclination angle

Type	Angle	Temperature	Peak power in Watts
Thin film	15	25°c-35°c	1080
	30		1160
	15	17°c-19°c	1080
	30		680
Polly crystalline	15	25°c-35°c	1020
	30		1140
	15	17°c-19°c	1040
	30		648
Mono-crystalline	15	25°c-35°c	860
	30		920
	15	17°c-19°c	900
	30		548

Result from **Table 2.** pertains to the impact of module type and operating conditions, such as module tilt and surrounding temperature, on the daily output of electric energy.

This influence is found to significantly affect the efficiency of the system. Nevertheless, the greatest amount of energy is derived from thin film modules. The performance of mono-crystalline modules and polycrystalline modules is nearly similar. The efficiency of a system may be influenced by variations in temperature and humidity within the range of 0 to 50%.

The efficiency of the system may potentially rise by a range of 10% to 25% when the inclination angle is increased from 15º to 30º. Furthermore, thin film photovoltaics (PV) have notable appeal as a method for constructing models.

In the optimization phase of this study, two methodologies were employed to obtain the optimal values for the variables of the LCL filter, specifically X = [L, Lg, Cf and fs]. The primary objective was to minimize the Levelized Cost of Energy (LCOE).

According to the trials, GA and WCA parameters, are given in **Table 3**. From trails the lower and upper bounds of the for LCL output filter are shown in **Table 4,**

Table 3: GA and WCA parameters

The parameter of GA and WCA	(L, Lg, Cf, and fs)
Population size	5
Number of generations	50

Table4: Range of LCL filter parameter

LCL filter parameter	Minimum value	Maximum value
L	1e-3	7.7e-3
Lg	1e-10	7.7e-3
Cf	6.570e-06	6.567e-6
fs	29500	30e3

A comparative analysis between the Genetic Algorithm (GA) and the Water Cycle Algorithm (WCA) was conducted, and the results were presented in **Table 5.**

Table 5. The optimal values of the PV inverter design variable for water cycle algorithm compared with Genetic algorithm.

Inverter connected to		**L (mH)**	**Lg (μH)**	**Cf (μF)**	**Fs (KHz)**	**LCOE (€/wh)**
Poly Crystalline	GA	1.1	288.055	6.134	29.7	1.0303
	WCA	1.5	91.822	6.166	29.6	0.7886
Mono Crystalline	GA	1.1	278.055	6.514	29.7	1.6229
	WCA	2.3	44.914	6.486	29.7	1.4852
Thin Films	GA	1.0	838.5	6.567	29.5	3.1466
	WCA	1.2	269.7	6.569	29.7	2.1648

The obtained data is presented in **Table 5**. The WCA technique demonstrates superior performance compared to the GA technique across several types of photovoltaic modules.

In addition, it is advisable to employ Polycrystalline modules for the purpose of achieving economic viability in PV systems. This recommendation is supported by the utilization of two approaches employed in the conducted test.

Following the obtained results, each inverter among the three inverters will be subjected to alternating testing with the remaining PV modules.

Table 6. Economical comparison results by trying each inverter from optimization results on the three types with the results.

Inverter /optimization technique		**Polycrystalline Modules**	**Mono-crystalline Modules**	**Thin film Modules**
Inverter connected to Poly-crystalline.	GA	1.0303	0.9710	1.6501
	WCA	0.7886	0.8886	1.1351
Inverter connected to Mono-crystalline.	GA	1.7219	1.6229	2.7574
	WCA	1.3180	1.4852	1.8971
Inverter connected to Thin film	GA	1.9648	1.8519	3.1466
	WCA	1.5040	1.6947	2.1648

From **Table 6.** the cost of the inverter which is connected to Polycrystllline modules applying GA is 1.0303 (€/wh) where the coast of it applying WCA is 0.7886 (€/wh). By using the inverter which connected to Polycrystalline modules to test it on Monocrystalline modoules gives coast 0.9710 (€/wh) with valuse of GA techniqes in **Table 6.** simmillary gives 0.8886 with value of WCA technique.Also for Thin Film modoules test with the same pattern gives 1.6501 (€/wh) for GA , and 1.1351 (€/wh) for WCA.That means the WCA alwayes gives better otptimal values than GA with all tyes under study.

Conclusion

This research undertook an evaluation of three distinct PV models, specifically polycrystalline, monocrystalline, and thin film, at their suitable inclination angles, accurately monitoring radiation and ambient temperature to compare their performance during summer and winter conditions over a span of two years (2021 and 2022). The study specifically focused on the effects of two distinct angles using diverse steel structures. The experimental setup involved positioning modules at a 15-degree angle throughout 2021 and at a 30-degree angle throughout 2022, facilitating a detailed comparative analysis. This study explains that a 15° inclination angle is superior to a 30° angle during winter, but a 30° inclination angle outperforms a 15° angle during summer. A comparative analysis has been conducted to examine the size of the output filter for inverters utilized in three different types of photovoltaic systems. This research employs GA and WCA to investigate the sizing aspects of the LCL output filter of the inverter. The WCA approach demonstrates superior performance compared to GA in optimizing solutions, specifically in terms of achieving optimal values for variables such as L, Lg, Cf, and Fs. The findings indicate that monocrystalline solar panels exhibit superior cost-effectiveness. The economic outcomes remain satisfactory even in the absence of any adjustments to the inverter settings. Additionally, the research investigated the critical aspect of determining the optimal size of the output filter inverter, with a primary focus on analyzing the LCOE. Recognizing the significance of LCOE in assessing the economic viability of renewable energy, this investigation not only enhances our understanding of PV module performance under varying conditions but also contributes valuable insights into optimizing the economic efficiency of solar energy.

Nomenclature

C_f	LCL-filter capacitor.
C_i	LCL-filter inductor cost per unit inductance and current rating.
C_{inv}	PV inverter Partial manufacturing cost.
C_m (X)	PV inverter Total manufacturing cost.
C_f	LCL-filter capacitor.
d_{max}	WCA Coefficient near to zero
E_y	Energy injected into the electric grid
f	Nominal frequency of the electric grid.
f_{sw}	Switching frequency.
$f_{sw,max}$	Maximum switching speed capability of the
$I_{o,t}$	Inverter output current at hour
I_r	The RMS value of the switching ripple due to the converter-side inductance.
L	Inverter inductance side
LB -UB	lower and upper boundaries
Lg	Grid inductance side
$P_{d,max}$	Maximum power dissipated in the damping resistor.
P_{tot}	Total power loss of the PV inverter.
P_{pv}	Output power of the PV array.
R_{dr}	LCL-filter damping resistor
V_n	Nominal voltage of the electric grid.
V_{pv}	Weighted average of the dc input voltage.

References

[1] W. Xiao, N. Ozog, and W. Dunford, "Topology study of photovoltaic interface for maximum power point tracking," IEEE Transactions on Industrial Electronics, vol. 54, no. 3, pp. 1696-1704, 2007.

[2] R. Singh, G. F. Alapatt, and A. Lakhtakia, "Making solar cells a reality in every home: Opportunities and challenges for photovoltaic device design," IEEE Journal of the Electron Devices Society, vol. 1, no. 6, pp. 129-144, 2013.

[3] A. Babatunde, S. Abbasoglu, and M. J. R. Senol, "Analysis of the impact of dust, tilt angle and orientation on performance of PV Plants," Renewable and Sustainable Energy Reviews, vol. 90, pp. 1017-1026, 2018.

[4] T. Kerekes, R. Teodorescu, P. Rodríguez, G. Vázquez, and E. Aldabas, "A new high-efficiency single-phase transformerless PV inverter topology," IEEE Transactions on industrial electronics, vol. 58, no. 1, pp. 184-191, 2009.

[5] M. A. Zaki, T. Mahmoud, M. Atia, and E. A. Osman, "OPTIMAL ALLOCATION OF CHARGING STATIONSFOR ELECTRICVEHICLE INDISTRIBUTIONSYSTEM USING ARTIFICIAL INTELLIGENCE TECHNIQUES," Journal of Al-Azhar University Engineering Sector, vol. 17, no. 65, pp. 1327-1347, 2022.

[6] O. Haillant, "Accelerated weathering testing principles to estimate the service life of organic PV modules," Solar Energy Materials and Solar Cells, vol. 95, no. 5, pp. 1284-1292, 2011.

[7] E. Figueres, G. Garcerá, J. Sandia, F. Gonzalez-Espin, and J. C. Rubio, "Sensitivity study of the dynamics of three-phase photovoltaic inverters with an LCL grid filter," IEEE Transactions on Industrial Electronics, vol. 56, no. 3, pp. 706-717, 2008.

[8] E. Koutroulis and F. Blaabjerg, "Design optimization of grid-connected PV inverters," in 2011 Twenty-Sixth Annual IEEE Applied Power Electronics Conference and Exposition (APEC), 2011, pp. 691-698: IEEE.

[9] B. M. Khaled, A. A. Attia, and O. Abdellatif, "EXPERIMENTAL STUDY ON CONVECTIVE HEAT TRANSFER USING FINS FOR COOLING PV CELLS," Journal of Al-Azhar University Engineering Sector, vol. 17, no. 65, pp. 1276-1289, 2022.

[10] H. El-Ghetany, M. Halawa, M. Mohammed, and I. Elmasry, "EXPERIMENTAL INVESTIGATION OF A MOBILE PV WATER PUMPING SYSTEM," Journal of Al-Azhar University Engineering Sector, vol. 17, no. 65, pp. 1290-1314, 2022.

[11] E. Koutroulis and F. Blaabjerg, "Techniques for the optimal design of photovoltaic inverters interconnected with the electric grid," in Proceedings of the 2011 14th European Conference on Power Electronics and Applications, 2011, pp. 1-10: IEEE.

[12] A. Balaska, A. Tahri, F. Tahri, and A. B. Stambouli, "Performance assessment of five different photovoltaic module technologies under outdoor conditions in Algeria," Renewable Energy, vol. 107, pp. 53-60, 2017.

[13] E. Lorenzo, Solar electricity: engineering of photovoltaic systems. Progensa, 1994.

[14] Y. Abou Jieb, E. Hossain, and E. Hossain, Photovoltaic systems: fundamentals and applications. Springer, 2022.

[15] S. K. Pattanaik and K. Mahapatra, "Power loss estimation for PWM and soft-switching inverter using RDCLI," International MultiConferene of Engineers and Computer Scientists (IMECS), vol. II, pp. 17-22, 2010.

[16] E. Koutroulis and F. Blaabjerg, "Design optimization of transformerless grid-connected PV inverters including reliability," IEEE Transactions on Power Electronics, vol. 28, no. 1, pp. 325-335, 2012.

[17] M. Liserre, F. Blaabjerg, and S. Hansen, "Design and Control of an LCL-Filter-Based Three-Phase Active Rectifier," IEEE Transactions on Industry Applications, vol. 41, no. 5, pp. 1281-1291, 2005.

[18] H. Eskandar, A. Sadollah, A. Bahreininejad, and M. Hamdi, "Water cycle algorithm–A novel metaheuristic optimization method for solving constrained engineering optimization problems," Computers Structures, vol. 110, pp. 151-166, 2012.

[19] S. A. Kannenberg, M. A. Sturchio, M. D. Venturas, and A. K. Knapp, "Grassland carbon-water cycling is minimally impacted by a photovoltaic array," Communications Earth Environment, vol. 4, no. 1, p. 238, 2023.

[20] A. Sadollah, H. Eskandar, H. M. Lee, and J. H. Kim, "Water cycle algorithm: a detailed standard code," SoftwareX, vol. 5, pp. 37-43, 2016.

[21] K. Krishnaram and T. Suresh Padmanabhan, "A Water Cycle Approach for Maximum Power Point Tracking through an Interleaved Boost Converter," Electric Power Components Systems, pp. 1-13, 2023.